Available online at www.sciencedirect.com
ScienceDirect
Journal of the European Ceramic Society 27 (2007) 813–817
www.elsevier.com/locate/jeurceramsoc

High-temperature thermoelectric properties of polycrystalline $Zn_{1-x-y}Al_xTi_yO$ ceramics

K. Park [a,*], K.Y. Ko [a], W.-S. Seo [b], W.-S. Cho [c], J.-G. Kim [d], J.Y. Kim [e]

[a] *Department of Advanced Materials Engineering, Sejong University, Seoul 143-747, Republic of Korea*
[b] *Korea Institute of Ceramic Engineering and Technology, Seoul 153-023, Republic of Korea*
[c] *School of Materials Science and Engineering, Inha University, Inchon 402-751, Republic of Korea*
[d] *Inorganic Chemistry Examination Division, Korean Intellectual Property Office, Daejeon 302-701, Republic of Korea*
[e] *Department of Advanced Materials Engineering, Hoseo University, Asan 336-795, Republic of Korea*

Available online 22 May 2006

Abstract

The as-sintered $Zn_{1-x}Al_xO$ ($0 \le x \le 0.05$) samples crystallized in the ZnO with a wurtzite structure, along with a small amount of the cubic spinel $ZnAl_2O_4$. The addition of Al_2O_3 to ZnO gave rise to a decrease in grain size, ranging from 7.3 to 2.7 μm and in relative density, ranging from 99.2 to 90.1% of the theoretical density. In the $Zn_{0.97}Al_{0.03-y}Ti_yO$ samples, as the amount of TiO_2 increased, the grain size of ZnO grains and second phases, such as Zn_2TiO_4 and $ZnAl_2O_4$, as well as density increased. The co-doping of Al and Ti led to a significant increase in both the electrical conductivity and the absolute value of the Seebeck coefficient, resulting in an increase in the power factor. The highest value of power factor (3.8×10^{-4} W m^{-1} K^{-2}) was attained for $Zn_{0.97}Al_{0.02}Ti_{0.01}O$ at 800 °C. It is demonstrated that the Al and Ti co-doping is fairly effective for enhancing thermoelectric properties.

Keywords: Powders-solid state reaction; Sintering; Electron microscopy; Electrical properties; TiO_2

1. Introduction

Thermoelectric materials have attracted significant interest as useful materials in the field of thermoelectric power generation and cooling devices. The performance of thermoelectric materials can be evaluated by the figure-of-merit (Z) defined as $Z = \sigma\alpha^2/\kappa$, where σ, α, and κ are the electrical conductivity, Seebeck coefficient, and thermal conductivity, respectively. With respect to high-temperature operation in air, metal oxides are generally advantageous owing to their excellent thermal and oxidation resistance. In particular, several p-type oxide systems, such as $NaCo_2O_4$ and $Ca_3Co_4O_9$, have been extensively studied so far.[1–6] Development of new oxide materials is still the most important issue for practical applications of thermoelectric power generation.

In this work, we have selected as a candidate material ZnO-based compounds. ZnO is an n-type semiconducting oxide with a wide direct band gap of 3.3 eV and has the wurtzite structure.[7] Recently, it becomes an outstandingly promising oxide material as a high-temperature thermoelectric material above 700 °C because of its high melting temperature (1800 °C), good chemical stability, high electrical conductivity, and high Seebeck coefficient.[8,9] It is well known that the addition of dopants is a feasible route to optimizing the thermoelectric performance. In the present work, we studied the microstructure and high-temperature thermoelectric properties of the $Zn_{1-x-y}Al_xTi_yO$ fabricated by a solid state reaction.

2. Experimental

All $Zn_{1-x-y}Al_xTi_yO$ ($0 \le x \le 0.05$, $0 \le y \le 0.02$) samples were fabricated by a solid state reaction starting from the high-purity ZnO, Al_2O_3, and TiO_2 powders. The mixture of the ZnO, Al_2O_3, and TiO_2 powders and ethyl alcohol was milled for 6 h using a planetary mill (FRITSCH pulverisette 6) and ZrO_2 as grinding media. The resulting slurries were dried at 80 °C in an oven for 24 h. The mixed powders were calcined in a mullite crucible at 1000 °C for 5 h. The calcined powders were milled in the planetary mill for 6 h and dried at 80 °C in an oven for 12 h. The dried powders were pressed using a hand press at a

* Corresponding author. Tel.: +82 2 3408 3777; fax: +82 2 3408 3664.
E-mail address: kspark@sejong.ac.kr (K. Park).

0955-2219/$ – see front matter © 2006 Elsevier Ltd. All rights reserved.
doi:10.1016/j.jeurceramsoc.2006.04.012

pressure of 98 MPa to prepare pellets of 5 mm thick and 20 mm diameter. The green compacts were heated at 1400 °C for 20 h in air and then furnace cooled.

The porosity of the as-sintered $Zn_{1-x-y}Al_xTi_yO$ samples was measured by the Archimedes principle. The crystalline structure of the as-sintered samples was analyzed with X-ray diffraction (XRD) (Rigaku RINT2000) using Cu Kα radiation at 40 kV and 100 mA. The microstructure of the as-sintered samples was investigated by using a scanning electron microscope (SEM) (Hitachi S4700). In order to identify the distribution of constituent elements in the as-sintered samples, secondary electron images (SEI) and elemental maps were acquired using an electron probe microanalysis (EPMA) attached on the SEM. In order to measure the thermoelectric properties as a function of temperature, the electrical conductivity (σ) and the Seebeck coefficient (α) were simultaneously measured over the temperature range from 450 up to 800 °C. The specimens for the measurements of thermoelectric properties were cut out of the sintered bodies in the form of rectangular bars of 2 mm × 2 mm × 15 mm with a diamond saw and polished with SiC emery papers. Four grooves were put on the rectangular bars. Pt wires were wound along the grooves. The holes (1.0 mm diameter) in the middle of the two end grooves of the specimens were machined. The insulated heads of the two Pt/Pt–Rh (13%) thermocouples were embedded in the two holes, and the temperature at the holes was measured. Electrical conductivity was measured by the direct current (d.c.) four-probe method. For thermopower measurements, a temperature difference in the specimen was generated by passing cool Ar gas over one end of the specimen placed inside a quartz protection tube. The temperature difference between the two ends in specimens was controlled to be 4–6 °C by varying the flowing rate of Ar gas. The thermopower (ΔE) measured as a function of the temperature difference (ΔT) gave a straight line. The Seebeck coefficient (α) was calculated from the relation $\alpha = \Delta E/\Delta T$.

3. Results and discussion

The as-sintered $Zn_{1-x}Al_xO$ ($0 \le x \le 0.05$) samples crystallized in the ZnO with a wurtzite structure, along with a small amount of the cubic spinel $ZnAl_2O_4$. The $ZnAl_2O_4$ phase was formed by the fact that the added Al_2O_3 (2–5 mol%) did not fully dissolve in the ZnO crystal lattice because of its limited solubility. The solubility of Al_2O_3 in ZnO is quite small, 0.01%.[10] The amount of the $ZnAl_2O_4$ increased with an increase in Al content. It has been reported that the $ZnAl_2O_4$ phase possesses a very low electrical conductivity.[11] In the $Zn_{0.97}Al_{0.03-y}Ti_yO$ samples, the substitution of Ti for Al gives rise to an increase in Zn_2TiO_4 and a decrease in $ZnAl_2O_4$. For example, the XRD patterns of the as-sintered $Zn_{0.97}Al_{0.03}O$, $Zn_{0.97}Al_{0.025}Ti_{0.005}O$, and $Zn_{0.97}Al_{0.01}Ti_{0.02}O$ are shown in Fig. 1(a)–(c), respectively. These results for the presence of the Zn_2TiO_4 and $ZnAl_2O_4$ phases in the sintered bodies are confirmed by SEI and elemental maps (Fig. 2).

Fig. 3 shows the SEM images from the surface of the as-sintered $Zn_{1-x-y}Al_xTi_yO$ samples. In the $Zn_{1-x}Al_xO$ samples, it is apparent that the addition of Al_2O_3 to ZnO gives rise to a decrease in the grain size, indicating that the added Al_2O_3

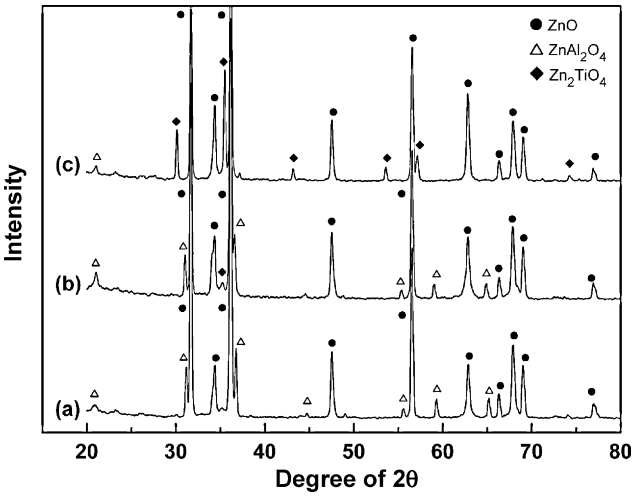

Fig. 1. XRD patterns of as-sintered (a) $Zn_{0.97}Al_{0.03}O$, (b) $Zn_{0.97}Al_{0.025}Ti_{0.005}O$, and (c) $Zn_{0.97}Al_{0.01}Ti_{0.02}O$ samples.

retarded the grain growth during sintering. This is attributed to the pinning effect caused by the $ZnAl_2O_4$ particles on grain boundaries and to the dragging effect between the added Al_2O_3 and grain boundaries, resulting in a reduction in the mobility of grain boundaries.[12,13] Fine $ZnAl_2O_4$ particles below ~1 μm in size are frequently dispersed on the grain boundaries of the ZnO matrix. In addition, the incorporation of Al_2O_3 to ZnO leads to a decrease in the density, ranging from 99.2 to 90.1% of the theoretical density. This is because the added Al_2O_3 acts to lower the grain-boundary mobility, thus enabling the pores to stay attached to the moving grain boundaries during sintering. A similar behavior was reported for Bi-doped ZnO.[13,14] The grain growth of ZnO in the presence of Bi_2O_3-rich phase has been hindered.

In the $Zn_{0.97}Al_{0.03-y}Ti_yO$ samples, it was found that the grain size and density of the ZnO matrix increased with increasing Ti content, indicating that sintering was promoted by the addition of TiO_2. This is because the added TiO_2 accelerates the mass transport of the $Zn_{0.97}Al_{0.03-y}Ti_yO$ samples. For example, the average grain sizes of the $Zn_{0.97}Al_{0.025}Ti_{0.005}O$ and $Zn_{0.97}Al_{0.01}Ti_{0.02}O$ samples were 4.1 and 7.6 μm, respectively, and the porosities of the $Zn_{0.97}Al_{0.025}Ti_{0.005}O$ and $Zn_{0.97}Al_{0.01}Ti_{0.02}O$ samples were 3.5 and 1.5%, respectively. TiO_2 is commonly used as the additive for enhancing the grain growth.[15–17] Most of the $ZnAl_2O_4$ and Zn_2TiO_4 particles exist on the grain boundaries of the ZnO matrix. The size of the two particles increased with TiO_2 content. The grain size and porosity of all the prepared $Zn_{1-x-y}Al_xTi_yO$ samples are given in Table 1.

The electrical conductivity as a function of temperature for the $Zn_{1-x-y}Al_xTi_yO$ samples is shown in Fig. 4. It is clear that the electrical conductivity increased with increasing temperature, indicating semiconducting behavior. In the $Zn_{1-x}Al_xO$ samples, the addition of a small amount of Al_2O_3 to ZnO leads to an increase in the conductivity. This is mainly attributed to the fact that the substitution of trivalent Al^{3+} for divalent Zn^{2+} increases the electron concentration of the system. The conductivity of $Zn_{0.95}Al_{0.05}O$ is slightly higher than that of $Zn_{0.97}Al_{0.03}O$. This

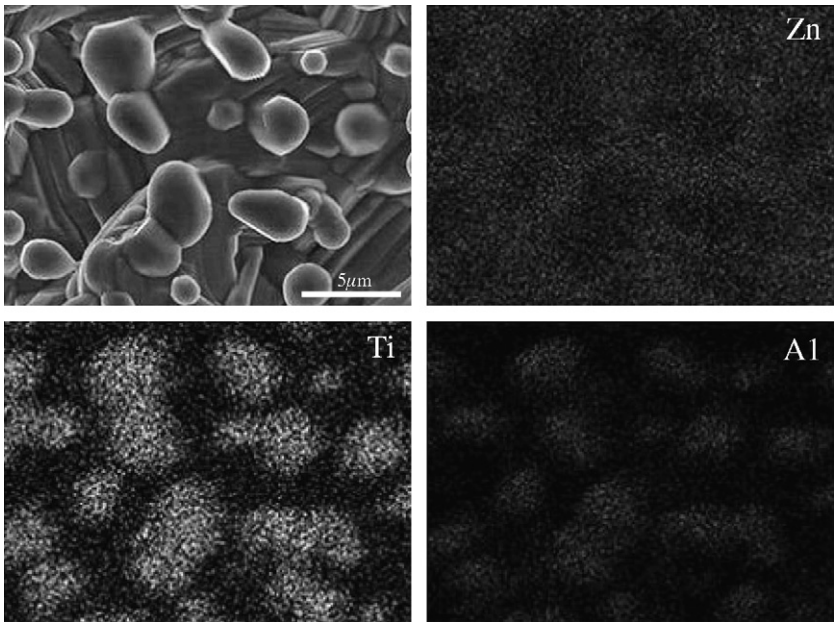

Fig. 2. SEI and elemental maps of as-sintered $Zn_{0.97}Al_{0.01}Ti_{0.02}O$ sample.

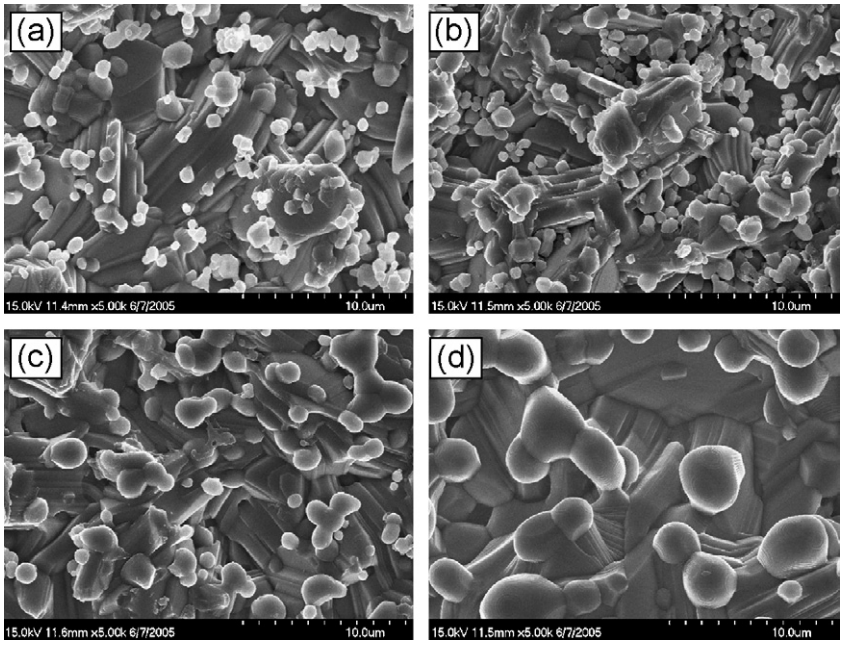

Fig. 3. SEM images from the surface of as-sintered (a) $Zn_{0.98}Al_{0.02}O$, (b) $Zn_{0.97}Al_{0.03}O$, (c) $Zn_{0.97}Al_{0.025}Ti_{0.005}O$, and (d) $Zn_{0.97}Al_{0.01}Ti_{0.02}O$ samples.

Table 1
Grain size and porosity of the prepared $Zn_{1-x-y}Al_xTi_yO$ samples

	Porosity (%)	Grain size (μm)
ZnO	0.8	7.3
$Zn_{0.98}Al_{0.02}O$	2.1	4.3
$Zn_{0.97}Al_{0.03}O$	4.5	3.8
$Zn_{0.95}Al_{0.05}O$	9.9	2.7
$Zn_{0.97}Al_{0.025}Ti_{0.005}O$	3.5	4.1
$Zn_{0.97}Al_{0.02}Ti_{0.01}O$	2.5	5.7
$Zn_{0.97}Al_{0.015}Ti_{0.015}O$	1.9	6.7
$Zn_{0.97}Al_{0.01}Ti_{0.02}O$	1.5	7.6

is because although the higher Al content gives rise to an increase in the conductivity, it results in a decrease in the density and grain size and in an increase in the amount of the $ZnAl_2O_4$ phase having a very low electrical conductivity. The decrease in the density and grain size is responsible for a decrease in the time between electron scattering events of charge carriers, thus decreasing the conductivity. It is also important to note that the substitution of Ti^{4+} for trivalent Al^{2+} in $Zn_{0.97}Al_{0.03}O$ significantly increases the electrical conductivity because of an increase in the electron concentrations, grain size, and density of the system. It is therefore believed that the co-doping of Al and Ti is fairly effective in achieving high conductivity.

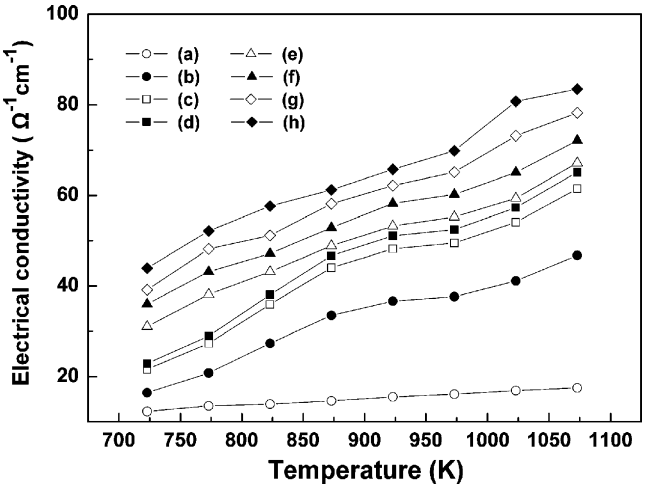

Fig. 4. Electrical conductivity as a function of temperature for (a) ZnO, (b) $Zn_{0.98}Al_{0.02}O$, (c) $Zn_{0.97}Al_{0.03}O$, (d) $Zn_{0.95}Al_{0.05}O$, (e) $Zn_{0.97}Al_{0.025}Ti_{0.005}O$, (f) $Zn_{0.97}Al_{0.02}Ti_{0.01}O$, (g) $Zn_{0.97}Al_{0.015}Ti_{0.015}O$, and (h) $Zn_{0.97}Al_{0.01}Ti_{0.02}O$ samples.

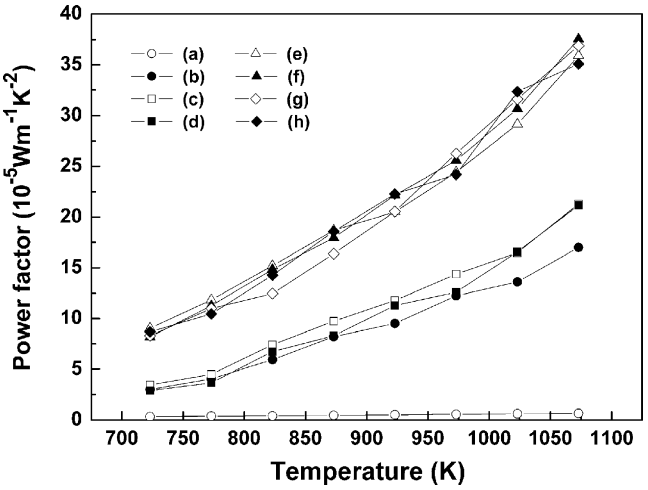

Fig. 6. Temperature dependence of the power factor for (a) ZnO, (b) $Zn_{0.98}Al_{0.02}O$, (c) $Zn_{0.97}Al_{0.03}O$, (d) $Zn_{0.95}Al_{0.05}O$, (e) $Zn_{0.97}Al_{0.025}Ti_{0.005}O$, (f) $Zn_{0.97}Al_{0.02}Ti_{0.01}O$, (g) $Zn_{0.97}Al_{0.015}Ti_{0.015}O$, and (h) $Zn_{0.97}Al_{0.01}Ti_{0.02}O$ samples.

Fig. 5 shows the temperature dependence of the Seebeck coefficient for the $Zn_{1-x-y}Al_xTi_yO$ samples. The sign of the Seebeck coefficient is negative over the whole temperature range for all the samples, indicating that the major conductivity carriers are electrons. In the $Zn_{1-x}Al_xO$ samples, the absolute value of the Seebeck coefficient decreased with increasing Al content mainly because of an increase in the electron concentration. This result qualitatively agrees with that based on the broad-band semiconducting model.[18] According to the broad-band model, the value of the Seebeck coefficient in common semiconductors decreases with increasing carrier density. Based on a simplified broad-band model, the Seebeck coefficient of the extrinsic n-type semiconductors with negligible hole conduction devices can be expressed as follows:[11] $\alpha = -(k/e)[\ln(N_v/n) + A]$, where k is the Boltzmann constant, n the electron concentration, e the electric charge of the carrier, N_v the density of state, and A is a transport constant typically $0 \le A \le 2$. In spite of the decrease in the Seebeck coefficient owing to an increase in the electron concentration, the absolute value of the Seebeck coefficient is still moderate as high as 180–191 $\mu V\,K^{-1}$ at 800 °C.

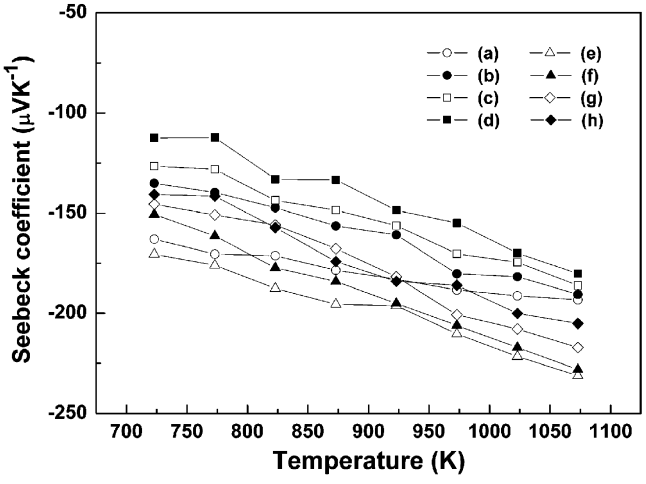

Fig. 5. Temperature dependence of the Seebeck coefficient for (a) ZnO, (b) $Zn_{0.98}Al_{0.02}O$, (c) $Zn_{0.97}Al_{0.03}O$, (d) $Zn_{0.95}Al_{0.05}O$, (e) $Zn_{0.97}Al_{0.025}Ti_{0.005}O$, (f) $Zn_{0.97}Al_{0.02}Ti_{0.01}O$, (g) $Zn_{0.97}Al_{0.015}Ti_{0.015}O$, and (h) $Zn_{0.97}Al_{0.01}Ti_{0.02}O$ samples.

In particular, it must be stressed that the absolute values of the Seebeck coefficient for the Ti-doped $Zn_{0.97}Al_{0.03-y}Ti_yO$ samples are much higher than those for the Ti-free $Zn_{1-x}Al_xO$ samples. The absolute values of the Seebeck coefficient for the Ti-doped $Zn_{0.97}Al_{0.03-y}Ti_yO$ samples range from 205 to 231 $\mu V\,K^{-1}$ at 800 °C. These results indicate that the conduction mechanism in the $Zn_{0.97}Al_{0.03-y}Ti_yO$ samples is not explained by the conventional broad-band model. We do not have detailed ideas to fully explain this behavior at present. To elucidate the detailed nature of the electrical conduction, further investigation is required, i.e., exact carrier concentrations, the Hall mobility, the effective mass, and the defect structure of the samples.

The temperature dependence of the power factor ($\sigma\alpha^2$) calculated from the data in Figs. 4 and 5 is plotted in Fig. 6. The power factor increased up to 800 °C. The power factors of the Ti-doped $Zn_{0.97}Al_{0.03-y}Ti_yO$ samples are extremely high, compared to the Ti-free $Zn_{1-x}Al_xO$ samples. $Zn_{0.97}Al_{0.02}Ti_{0.01}O$ showed the highest value of power factor ($3.8 \times 10^{-4}\,W\,m^{-1}\,K^{-2}$) at 800 °C. In addition to their high power factors, the Ti-substituted $Zn_{0.97}Al_{0.03-y}Ti_yO$ ceramics have several inherent advantages for use in thermoelectric devices, i.e., excellent chemical stability under oxidizing atmospheres at high temperatures. Summarizing the aforementioned results, it may be believed that polycrystalline $Zn_{1-x-y}Al_xTi_yO$ could be promising for thermoelectric applications at high temperatures.

4. Conclusions

Polycrystalline $Zn_{1-x-y}Al_xTi_yO$ ($0 \le x \le 0.05$, $0 \le y \le 0.02$) samples were fabricated by a solid state reaction method. The as-sintered $Zn_{1-x}Al_xO$ ($0 \le x \le 0.05$) samples crystallized in the

ZnO with a wurtzite structure, along with a small amount of the cubic spinel $ZnAl_2O_4$. The amount of the $ZnAl_2O_4$ increased with an increase in Al content. The grain size decreased with increasing Al content because of the pinning effect caused by the $ZnAl_2O_4$ particles on grain boundaries and to the dragging effect between the added Al_2O_3 and grain boundaries. The added Al_2O_3 gave rise to a decrease in the density, ranging from 99.2 to 90.1% of the theoretical density. In addition, the substitution of Ti for Al in $Zn_{0.97}Al_{0.03}O$ led to an increase in Zn_2TiO_4 and a decrease in $ZnAl_2O_4$. The grain size and density of the $Zn_{0.97}Al_{0.03-y}Ti_yO$ samples increased with increasing Ti content, indicating that sintering was promoted by the addition of TiO_2.

In particular, the electrical conductivity (σ) and the absolute value of the Seebeck coefficient (α) for the Ti-doped $Zn_{0.97}Al_{0.03-y}Ti_yO$ samples were much higher than those for the Ti-free $Zn_{1-x}Al_xO$ samples. The higher electrical conductivity was caused by the increased extra electrons, grain size, and density of the system. The power factors ($\sigma\alpha^2$) of the Ti-doped $Zn_{0.07-y}Al_{0.03}Ti_yO$ samples were extremely high, compared to the Ti-free $Zn_{1-x}Al_xO$ samples. $Zn_{0.97}Al_{0.02}Ti_{0.01}O$ showed the highest value of power factor ($3.8 \times 10^{-4}\,W\,m^{-1}\,K^{-2}$) at 800 °C. It is strongly believed that the co-doping of Al and Ti is fairly effective for enhancing thermoelectric properties.

Acknowledgement

The authors would like to acknowledge the financial support provided for this research by the Korea Energy Management Corporation (KEMCO).

References

1. Terasaki, I., Sasago, Y. and Uchinokura, K., Large thermoelectric power in $NaCo_2O_4$ single crystals. *Phys. Rev. B*, 1997, **56**, R12685–R12687.
2. Terasaki, I., Transport properties and electronic states of the thermoelectric oxide $NaCo_2O_4$. *Phys. B*, 2003, **328**, 63–67.
3. Fujita, K., Mochida, T. and Nakamura, K., High-temperature thermoelectric properties of $Na_xCoO_{2-\delta}$ single crystals. *Jpn. J. Appl. Phys.*, 2001, **40**, 4644–4647.
4. Terasaki, I., Cobalt oxides and Kondo semiconductors: a pseudogap system as a thermoelectric material. *Mater. Trans.*, 2001, **42**, 951–955.
5. Ando, Y., Miyamoto, N., Segawa, K., Kawata, T. and Terasaki, I., Specific-heat evidence for strong electron correlations in the thermoelectric material (Na, Ca)Co_2O_4. *Phys. Rev. B*, 1999, **60**, 10580–10583.
6. Masuda, Y., Nagahama, D., Itahara, H., Tani, T., Seo, W. S. and Koumoto, K., Thermoelectric performance of Bi- and Na-substituted $Ca_3Co_4O_9$ improved through ceramic texturing. *J. Mater. Chem.*, 2003, **13**, 1094–1099.
7. Shan, F. K. and Yu, Y. S., Band gap energy of pure and Al-doped ZnO thin films. *J. Eur. Ceram. Soc.*, 2004, **24**, 1869–1872.
8. Kazeoka, M., Hiramatsu, H., Seo, W. S. and Koumoto, K., Improvement in thermoelectric properties of $(ZnO)_5In_2O_3$ through partial substitution of ytrium for indium. *J. Mater. Chem.*, 1998, **13**, 523–526.
9. Maeda, H., Nakao, Y. and Hojo, J., Thermoelectric properties of ZnO-Al_2O_3 ceramics. In *Proceedings of the 17th International Conference on Thermoelectrics*, 1998, pp. 614–617.
10. Katsuyama, S., Takagi, Y., Ito, M., Majima, K., Nagai, H., Sakai, H., Yoshimura, K. and Kosuge, K., Thermoelectric properties of $(Zn_{1-y}Mg_y)_{1-x}Al_xO$ ceramics prepared by the polymerized complex method. *J. Appl. Phys.*, 2002, **92**, 1391–1398.
11. Ohtaki, M., Tsubota, T., Eguchi, K. and Arai, H., High-temperature thermoelectric properties of $(Zn_{1-x}Al_x)O$. *J. Appl. Phys.*, 1996, **79**, 1816–1818.
12. Bernik, S., Daneu, N. and Rečnik, A., Inversion boundary induced grain growth in TiO_2 or Sb_2O_3 doped ZnO-based varistor ceramics. *J. Eur. Ceram. Soc.*, 2004, **24**, 3703–3708.
13. Cotterill, P. and Mould, P. R., *Recrystallization and Grain Growth in Metals*. John Wiley & Sons, New York, 1976, pp. 150–163.
14. Senda, T. and Bradt, R. C., Grain growth in sintered ZnO and ZnO–Bi_2O_3 ceramics. *J. Am. Ceram. Soc.*, 1990, **73**, 106–114.
15. Dey, D. and Bradt, R. C., Grain growth of ZnO during Bi_2O_3 liquid-phase sintering. *J. Am. Ceram. Soc.*, 1992, **75**, 2529–2534.
16. Peigney, A., Andrianjatovo, H., Legros, R. and Rousset, A., Influence of chemical composition on sintering of bismuth–titanium-doped zinc oxide. *J. Mater. Sci.*, 1992, **27**, 2397–2405.
17. Suzuki, H. and Bradt, R. C., Grain growth of ZnO in ZnO–Bi_2O_3 ceramics with TiO_2 additions. *J. Am. Ceram. Soc.*, 1995, **78**, 1354–1360.
18. Bhandari, C. M. and Rowe, D. M., Optimization of carrier concentration. In *CRC Handbook of Thermoelectrics*, ed. D. M. Rowe. CRC Press, Boca Raton, 1995, pp. 43–46.